LETTER

doi:10.1038/nature10072

Detection of prokaryotic mRNA signifies microbial viability and promotes immunity

Leif E. Sander[1], Michael J. Davis[2]*, Mark V. Boekschoten[3]*, Derk Amsen[4], Christopher C. Dascher[1], Bernard Ryffel[5], Joel A. Swanson[2], Michael Müller[3] & J. Magarian Blander[1]

Live vaccines have long been known to trigger far more vigorous immune responses than their killed counterparts[1–6]. This has been attributed to the ability of live microorganisms to replicate and express specialized virulence factors that facilitate invasion and infection of their hosts[7]. However, protective immunization can often be achieved with a single injection of live, but not dead, attenuated microorganisms stripped of their virulence factors. Pathogen-associated molecular patterns (PAMPs), which are detected by the immune system[8,9], are present in both live and killed vaccines, indicating that certain poorly characterized aspects of live microorganisms, not incorporated in dead vaccines, are particularly effective at inducing protective immunity. Here we show that the mammalian innate immune system can directly sense microbial viability through detection of a special class of viability-associated PAMPs (vita-PAMPs). We identify prokaryotic messenger RNA as a vita-PAMP present only in viable bacteria, the recognition of which elicits a unique innate response and a robust adaptive antibody response. Notably, the innate response evoked by viability and prokaryotic mRNA was thus far considered to be reserved for pathogenic bacteria, but we show that even non-pathogenic bacteria in sterile tissues can trigger similar responses, provided that they are alive. Thus, the immune system actively gauges the infectious risk by searching PAMPs for signatures of microbial life and thus infectivity. Detection of vita-PAMPs triggers a state of alert not warranted for dead bacteria. Vaccine formulations that incorporate vita-PAMPs could thus combine the superior protection of live vaccines with the safety of dead vaccines.

We hypothesized that the innate immune system might sense the most fundamental characteristic of microbial infectivity, microbial viability itself, and activate a robust immune response regardless of the presence of more specialized factors that regulate microbial virulence[7]. To study the sensing of bacterial viability without the compounding effects of replication or virulence factors, we used thymidine auxotrophs of non-pathogenic *Escherichia coli* K12, strain DH5α (hereafter called *thyA*$^-$ *E. coli*). Viable and heat-killed *thyA*$^-$ *E. coli* similarly activated nuclear factor-κB (NF-κB) and mitogen-activated protein kinase p38 (Supplementary Fig. 1) in murine bone-marrow-derived macrophages and elicited production of similar amounts of interleukin-6 (IL-6) and tumour necrosis factor-α (TNF-α) (Fig. 1a). In contrast, viable *thyA*$^-$ *E. coli* induced higher levels of IFN-β than heat-killed *thyA*$^-$ *E. coli* or lipopolysaccharide (LPS) (Fig. 1b), and only viable *thyA*$^-$ *E. coli* induced IL-1β secretion (Fig. 1c and Supplementary Fig. 2). Pro-IL-1β transcription was equally induced by both viable and heat-killed *thyA*$^-$ *E. coli* (Fig. 1c), indicating that viable bacteria specifically elicit cleavage of pro-IL-1β. This process is catalysed by caspase-1 in Nod-like receptor (NLR)-containing inflammasome complexes, the assembly of which can be triggered by the activity of bacterial virulence factors[10,11]. Notably, avirulent viable but not heat-killed *thyA*$^-$ *E. coli* induced inflammasome activation and pro-caspase-1 cleavage (Fig. 1d). Finally, viable but not heat-killed *thyA*$^-$ *E. coli* induced caspase-1-dependent inflammatory cell death, termed pyroptosis[10,11], resulting in the release of lactate dehydrogenase (LDH) (Fig. 1e) and the appearance of 7-amino-actinomycin D (7AAD)$^+$annexin-V$^{-/low}$ cells (Fig. 1f). Similar responses were observed in peritoneal macrophages and both splenic and bone-marrow-derived dendritic cells (Supplementary Fig. 2b). Killing *thyA*$^-$ *E. coli* by ultraviolet irradiation, antibiotics, or ethanol also selectively abrogated IL-1β secretion and pyroptosis without affecting IL-6 production (Fig. 1g and Supplementary Fig. 3), indicating that a general determinant associated with bacterial viability is detected.

To determine whether pathogenic bacteria can also activate the inflammasome in the absence of virulence factors, we studied attenuated strains of selected pathogens: *Shigella flexneri* virulence plasmid-cured strain BS103[12], *Salmonella enterica* serovar Typhimurium SL1344 Δ*Spi1*Δ*Spi2*, lacking the *Salmonella* pathogenicity islands SPI-1 and SPI-2 (ref. 10), and *Listeria monocytogenes* Δ*Hly*Δ*fliC*, lacking listeriolysin O and flagellin[10]. These mutants induced IL-1β production at levels comparable to those induced by *thyA*$^-$ *E. coli* (Fig. 1h), but lower and with slower kinetics than their pathogenic counterparts (Supplementary Fig. 4). IL-1β production was abolished when these bacteria were killed, whereas IL-6 production was similar (Fig. 1h). Thus, immune cells detect universal characteristics of viability different from virulence factors.

Caspase-1 activation, pyroptosis and IL-1β production in response to *thyA*$^-$ *E. coli* were abrogated in macrophages deficient for NLRP3 or for the inflammasome adaptor apoptosis speck protein with caspase recruitment (ASC or PYCARD)[11] (Fig. 1i, j), whereas NLRC4 was dispensable (Supplementary Fig. 5). Pyroptosis and IL-1β production induced by viable *thyA*$^-$ *E. coli* were abrogated in *Casp1*$^{-/-}$ macrophages (Fig. 1j) and suppressed by inhibitors for caspase-1, but not caspase-8 (Supplementary Fig. 6).

Induction of IFN-β mRNA and protein by viable *thyA*$^-$ *E. coli* required the Toll-like receptor (TLR) adaptor TRIF[9] (Fig. 2a, b) and downstream interferon regulatory factor-3 (IRF3)[9] (Supplementary Fig. 7), but not MyD88, the main TLR adaptor[9] (Fig. 2a, b). In contrast, transcription of pro-IL-1β was largely dependent on MyD88. Consequently, *Myd88*$^{-/-}$ cells secreted no IL-1β (Fig. 2c, d), whereas pyroptosis and caspase-1 cleavage were intact (Fig. 2e, f). Notably, although TRIF was dispensable for pro-IL-1β transcription (Fig. 2c), *Trif*$^{-/-}$ cells failed to secrete IL-1β (Fig. 2d), were protected from pyroptosis (Fig. 2e) and did not activate caspase-1 (Fig. 2f). These findings revealed an unexpected role for TRIF in NLRP3 inflammasome activation in response to viable *thyA*$^-$ *E. coli*. In contrast, pyroptosis induced by pathogenic *S. enterica* Typhimurium[10] proceeded independently of TRIF (Supplementary Fig. 8). Differential involvement of TRIF, together with differences in magnitude and kinetics of the response (Fig. 1h and Supplementary Fig. 4), indicated that inflammasome activation in

[1]Immunology Institute, Department of Medicine, Mount Sinai School of Medicine, 1425 Madison Avenue, New York, New York 10029, USA. [2]Department of Microbiology and Immunology, University of Michigan, Ann Arbor, Michigan 48109-0620, USA. [3]Nutrition, Metabolism and Genomics Group, Division of Human Nutrition, Wageningen University, 6703 HD Wageningen, The Netherlands. [4]Department of Cell Biology and Histology, Academic Medical Center, University of Amsterdam, 1105 AZ Amsterdam, The Netherlands. [5]Laboratory of Molecular Immunology and Embryology, University of Orleans and Centre National de la Recherche Scientifique, 45071 Orleans, France.

*These authors contributed equally to this work.

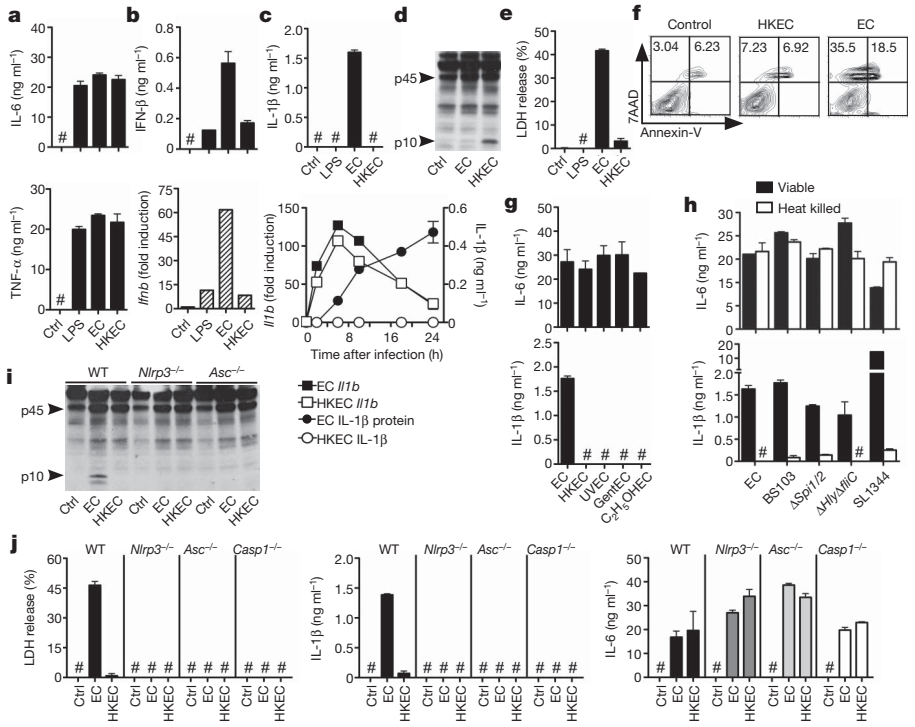

Figure 1 | Sensing bacterial viability induces IFN-β and activates the NLRP3 inflammasome in the absence of virulence factors. **a**, **b**, IL-6 and TNF-α (**a**) and IFN-β protein and mRNA (at 2 h) (**b**) levels in murine BMMs stimulated with medium (ctrl), lipopolysaccharide (LPS), *thyA*$^-$ *E. coli* (EC) and heat-killed *thyA*$^-$ *E. coli* (HKEC). Multiplicity of infection = 20. **c**, IL-1β (top), *Il1b* mRNA (bottom, left *y* axis) and secreted IL-1β (bottom, right *y* axis) at indicated times is shown. **d**, **i**, Caspase-1 immunoblots at 18 h in wild-type (**d**) or wild-type (WT), *Nlrp3*$^{-/-}$ and *Asc*$^{-/-}$ BMMs (**i**). **e**, **f**, Pyroptosis by LDH release (**e**) and FACS (**f**) at 18 h is shown. **g**, **h**, IL-6 and IL-1β in response to *thyA*$^-$ *E. coli*, viable or killed by different means (**g**, bone-marrow-derived dendritic cells (BMDCs)) or viable or heat-killed *thyA*$^-$ *E. coli*, attenuated *thyA*$^-$ *Shigella* (BS103), *Salmonella* (Δ*Spi1/2*) and *Listeria* (Δ*Hly*Δ*fliC*), or virulent *Salmonella* SL1344 (**h**). C_2H_5OHEC, ethanol-killed *E. coli*; GentEC, gentamicin-killed *E. coli*; UVEC, UV irradiated *E. coli*. **j**, LDH, IL-1β and IL-6 in BMMs of the indicated genotype in response to medium (ctrl), viable *thyA*$^-$ *E. coli* (EC) and heat-killed *thyA*$^-$ *E. coli* (HKEC). All responses are by murine BMMs and measured at 24 h unless indicated otherwise. Hash symbol indicates not detected. Data represent ≥5 experiments. All bars represent mean ± s.e.m.

response to virulence factors occurs in a manner distinct from that to viability.

Genome-wide transcriptional analysis of wild-type and *Trif*$^{-/-}$ macrophages before and after phagocytosis of viable *thyA*$^-$ *E. coli* showed differential regulation of several clusters of genes (Supplementary Fig. 9) including IFN-regulated genes, as expected[9] (Fig. 2a, b and Supplementary Fig. 10a), whereas most of the Rel/NF-κB target genes were comparable (Supplementary Fig. 10b). *Nlrp3* expression was induced independently of TRIF (Fig. 2g, h), and negative regulators of inflammasome activity, such as those encoded by Mediterranean fever (*Mefv*), *Nlrp10* and *Casp12* genes, were also unchanged or expressed at higher levels in wild-type macrophages (Fig. 2g), possibly due to negative feedback. Thus, the role of TRIF in inflammasome activation upon phagocytosis of viable *thyA*$^-$ *E. coli* is not explained by transcriptional control of inflammasome components (so called priming[11]). Furthermore, ATP and reactive oxygen species (ROS)[11,13], known activators of the NLRP3 inflammasome, were not involved, as deficiency for P_2X_7R, which is required for ATP-mediated NLRP3 activation, did not affect pyroptosis or IL-1β production (Supplementary Fig. 11a, b), and ROS accumulated equally in response to viable and heat-killed *thyA*$^-$ *E. coli* independently of TRIF (Supplementary Fig. 11c).

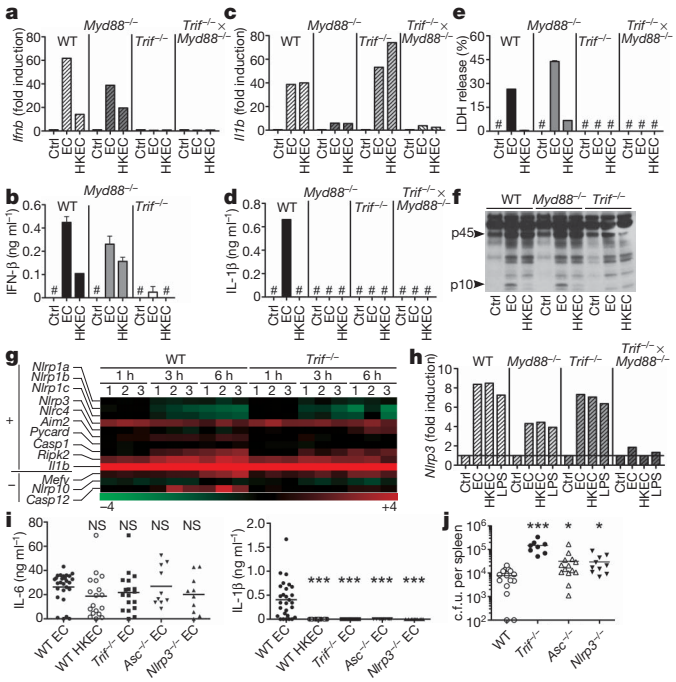

Figure 2 | The TLR signalling adaptor TRIF controls 'viability-induced' responses. **a**–**e**, *Ifnb* transcription at 2 h (**a**), IFN-β secretion at 24 h (**b**), *Il1b* transcription at 2 h (**c**), IL-1β secretion (**d**) and LDH release (**e**) at 24 h after phagocytosis of viable (EC) or heat-killed (HKEC) *thyA*$^-$ *E. coli*. **f**, Caspase-1 immunoblot at 18 h. Data in **a**–**f** are from murine BMMs and represent ≥5 experiments. **g**, Gene microarray analysis of wild-type and *Trif*$^{-/-}$ BMMs treated with viable *thyA*$^-$ *E. coli* for 1, 3 or 6 h (three biological replicates, numbered 1–3). A heat map of positive regulators/essential components (+) and negative regulators (−) of inflammasomes is shown. **h**, *Nlrp3* transcription at 1 h in BMMs. **i**, **j**, Serum levels of IL-6 and IL-1β 6 h after injection of 1×10^9 viable or 5×10^9 heat-killed *thyA*$^-$ *E. coli* (**i**), and splenic bacterial burdens 72 h after injection of 1×10^8 non-auxotroph *E. coli* (**j**) into wild-type, *Trif*$^{-/-}$, *Asc*$^{-/-}$ and *Nlrp3*$^{-/-}$ mice are shown. Each symbol represents one mouse. *, $P \leq 0.05$; **, $P \leq 0.01$; ***, $P \leq 0.001$. NS, not statistically significant. Hash symbol indicates not detected. All bars represent mean ± s.e.m.

Injection of viable and heat-killed *thyA*$^-$ *E. coli* into mice induced similarly high serum levels of IL-6 (Fig. 2i). In contrast, circulating IL-1β was detected only in mice infected with viable bacteria (Fig. 2i), whereas IFN-β levels were undetectable in all groups (data not shown). Confirming our results *in vitro*, production of IL-1β (but not IL-6) *in vivo* also required TRIF, ASC and NLRP3 (Fig. 2i). Injection of non-pathogenic *S. enterica* Typhimurium induced serum IL-1β levels comparable to those elicited by *thyA*$^-$ *E. coli*, which similarly depended on TRIF (Supplementary Fig. 12). Although pathogenic *S. enterica* Typhimurium elicited higher levels of serum IL-1β than non-pathogenic *Salmonella*, this response was also severely reduced in *Trif*$^{-/-}$ mice, suggesting a previously unappreciated role for TRIF in *Salmonella* infection (Supplementary Fig. 12). Importantly, deficiency in TRIF, ASC and NLRP3 impaired bacterial clearance during systemic infection with replication-sufficient non-pathogenic *E. coli* (Fig. 2j). This failure was more dramatic in *Trif*$^{-/-}$ than in *Asc*$^{-/-}$ or *Nlrp3*$^{-/-}$ mice, possibly due to the central upstream role of TRIF in inflammasome activation and IFN-β production.

The ability to sense microbial viability through pathways downstream of pattern recognition receptors indicates the existence of vita-PAMPs; that is, PAMPs associated with viable but not dead bacteria. In contrast to LPS and genomic DNA, which remained constant after killing *thyA*$^-$ *E. coli* with heat, total bacterial RNA was rapidly lost (Fig. 3a, b and Supplementary Fig. 13). Total RNA content was also lost with antibiotic treatment, and little ribosomal RNA (rRNA) remained after killing with ultraviolet irradiation and ethanol (Supplementary Fig. 14). Only fixation with paraformaldehyde (PFA) efficiently killed the bacteria (not shown) while preserving total RNA content (Supplementary Fig. 15a). Remarkably, unlike bacteria killed by other means, PFA-killed bacteria induced pyroptosis and IL-1β production to levels similar to those induced by viable bacteria (Supplementary Fig. 15b). Thus, the presence or absence of RNA correlated with the ability to activate pathways involved in sensing viability.

These results indicate that prokaryotic RNA represents a labile PAMP closely associated with bacterial viability that might signify microbial life to the immune system. Indeed, addition of purified total bacterial RNA fully restored the ability of heat-killed *thyA*$^-$ *E. coli* to induce pyroptosis, IL-1β and IFN-β production (Fig. 3c). These responses were dependent on TRIF, NLRP3 and caspase-1, just as those responses elicited by viable bacteria (Fig. 3d compared to Figs 1j and 2a–f). The NLRP3 inflammasome mediates recognition of viral RNA during influenza A infection[14]. Together with our results and those of others[15], this suggests a more general role for NLRP3 in responses to RNAs of microbial origin. RNA can activate the NLRP3 inflammasome when delivered into the cytosol (where NLRP3 is found) with transfection reagents[15]. In contrast, inflammasome activation by the combination of total bacterial RNA and dead *thyA*$^-$ *E. coli* did not require RNA transfection (Fig. 3c, d). Administration of total *E. coli* RNA alone or in combination with LPS (to mimic an *E.-coli*-derived PAMP plus RNA) had little effect on NLRP3 inflammasome activation unless the RNA was delivered to the cytosol using Lipofectamine (Supplementary Fig. 16) or in combination with ATP, as reported previously[15]. Thus, phagocytosis of viable bacteria is a natural context of bacterial-RNA-mediated NLRP3 inflammasome activation.

These findings raised the question as to how vita-PAMPs in phagolysosomes gain access to cytosolic receptors such as NLRP3 in the absence of invasion, auxiliary secretion systems or pore-forming toxins. To address this question, we exploited the pH-sensitive excitation spectrum of fluorescein: the acidic pH in phagolysosomes quenches fluorescence whereas release into the pH-neutral cytosol allows a regain in fluorescence[16]. Phagocytosis of avirulent *thyA*$^-$ *E. coli* in the presence of fluorescein-conjugated dextran (Fdx) consistently induced low-level release of Fdx into the cytosol of macrophages (Fig. 3e, f and Supplementary Fig. 17). This indicates that phagosomes carrying *E. coli* exhibit intrinsic leakiness, a property previously described for particles such as beads and crystals that induce phagolysosomal destabilization[16,17]. Interestingly, killed *E. coli* also induced Fdx release, although to a slightly lower extent than viable *E. coli* (Fig. 3e, f), demonstrating that phagosomal leakage occurs independently of bacterial viability. Therefore, RNA from viable

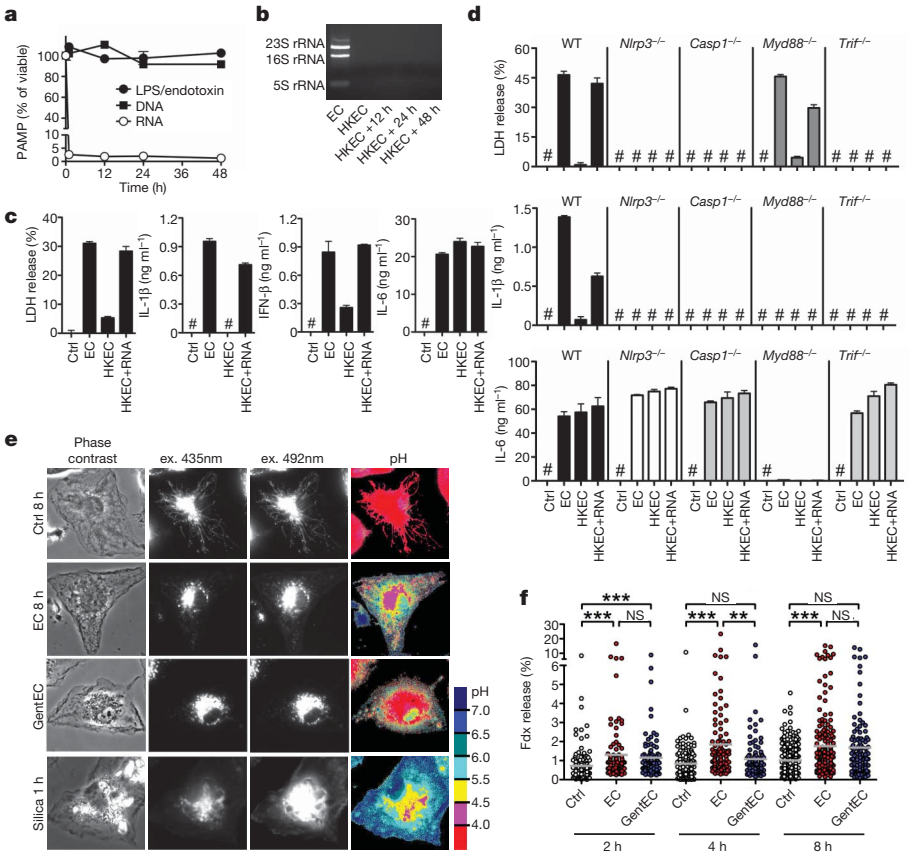

Figure 3 | Bacterial RNA is a vita-PAMP that accesses cytosolic receptors during phagocytosis and in the absence of virulence factors. **a**, LPS/endotoxin, genomic DNA and total RNA in *thyA*$^-$ *E. coli* before and at indicated times after heat killing. **b**, Agarose gel electrophoresis of *thyA*$^-$ *E. coli* total RNA before and after heat killing at 60 °C for 60 min followed by 4 °C incubation for the indicated times. **c**, **d**, LDH, IL-1β, IFN-β and IL-6 at 24 h in response to viable *thyA*$^-$ *E. coli* (EC), heat-killed *thyA*$^-$ *E. coli* (HKEC), or heat-killed *thyA*$^-$ *E. coli* with 10 μg ml^{-1} total RNA (HKEC+RNA). Hash symbol in **c** and **d** indicates not detected. Data in **a**–**d** are from murine BMMs and represent ≥5 experiments. **e**, Representative ratiometric epifluorescence imaging of murine BMMs at 8 h with Fdx alone (ctrl 8 h), Fdx and viable *thyA*$^-$ *E. coli* (EC 8 h) or gentamicin-killed *thyA*$^-$ *E. coli* (GentEC). Colour code indicates pH scale. Positive control is ground silica (silica 1 h). **f**, Quantification of cytosolic Fdx expressed as percentage of total Fdx per cell. Each dot represents the percentage of released Fdx per individual cell. Grey bars represent mean Fdx release. *, $P \leq 0.05$; **$P \leq 0.01$; ***, $P \leq 0.001$. All bars represent mean ± s.e.m.

bacteria could gain access to cytosolic receptors via intrinsic phagosomal leakage. These results may also explain the reported ability of phagosome-degraded mutants of *Listeria monocytogenes* or *Staphylococcus aureus* to induce a transcriptional response dependent on cytosolic NLRs[18,19].

Digestion of total RNA from *E. coli* with exonuclease RNase I and double-stranded RNA (dsRNA)-specific endonuclease RNase III abrogated LDH and IL-1β release, whereas DNase treatment had no effect (Fig. 4a). Of the *E. coli* RNA species, mRNA most potently induced pyroptosis as well as production of IL-1β and IFN-β. Small RNA (sRNA), or the most abundant RNA, ribosomal RNA (rRNA), had little or no detectable effects (Fig. 4b and Supplementary Fig. 18). *Escherichia coli* rRNA undergoes extensive modifications not found in mRNA[20], which may underlie the differential activity of these RNA species. The relative amount of mRNA was <1% of the total RNA and accordingly, mRNA was approximately 100-fold more effective than total RNA (Figs 3c and 4a, b and Supplementary Fig. 18).

In-vitro-transcribed single-stranded mRNA of the *E. coli* Gro operon (Supplementary Fig. 19a, b), which is strongly expressed upon phagocytosis of bacteria[21], induced caspase-1 cleavage and subsequent pyroptosis and IL-1β production when phagocytosed together with heat-killed *thyA*$^-$ *E. coli* (Fig. 4c, e and Supplementary Fig. 19c–e). The single-stranded Gro mRNA sequence had a predicted secondary structure with regions of high probability for base pairing (Fig. 4d), consistent with susceptibility of the stimulatory activity to RNase III treatment (Fig. 4a). Indeed, fully dsGro mRNA (Supplementary Fig. 19b) induced responses similar to single-stranded Gro mRNA of the appropriate length (Fig. 4e and Supplementary Fig. 19d). Other transcripts also induced such responses, showing that the immunostimulatory property is independent of RNA sequence (Fig. 4f).

Notably, eukaryotic RNA was unable to elicit the responses induced by *E. coli* mRNA (Fig. 4b). Unlike eukaryotic mRNA, triphosphate moieties at the 5′ end of bacterial mRNAs are not capped with 7-methyl-guanosine ($7m^7G$)[22], and might betray the prokaryotic origin of these transcripts[23]. However, neither treatment with calf intestinal phosphatase (CIP) nor capping affected the activity of Gro mRNA during phagocytosis of heat-killed *thyA*$^-$ *E. coli* (Fig. 4g). The stimulatory activity of purified *E. coli* total RNA or mRNA was also unaltered by CIP treatment (Supplementary Fig. 20a, b), arguing against a role for the RNA helicase retinoic acid inducible gene-I (RIG-I), which can induce interferon and IL-1β production but requires 5′-triphosphates for activation (Supplementary Fig. 20c)[23]. Moreover, TRIF and NLRP3 are dispensable for RIG-I function but are required for the stimulatory activity of bacterial RNA (Figs 2a, b and 3d). Interestingly, RNA can induce RIG-I-dependent IFN-β during infection with an invasive intracellular bacterium[24], indicating that the nature of microbial pathogenesis and the cellular context in which bacterial RNA is recognized may determine the choice of innate sensors engaged. In contrast to 5′-triphosphate removal, adding polyadenylyl groups to the 3′ end of Gro mRNA or purified *E. coli* mRNA abrogated IL-1β secretion and pyroptosis (Fig. 4g and Supplementary Fig. 21). Thus, absence of 3′-polyadenylation[22] may allow specific detection of prokaryotic mRNA during infection. Additional features may distinguish self from microbial RNAs such as internal naturally occurring nucleoside modifications in eukaryotic RNA[25–27].

To test the impact of vita-PAMPs on adaptive immunity, we immunized mice with either viable or dead *thyA*$^-$ *E. coli*, or a combination of dead *thyA*$^-$ *E. coli* and purified total bacterial RNA (Supplementary Fig. 22). Whereas all three vaccines induced similar polyclonal anti-*E. coli* IgM responses, production of class-switched IgG subclasses was strongly enhanced in response to vaccination with viable compared to killed *E. coli* (Fig. 4h). Adding total bacterial RNA to killed *thyA*$^-$ *E. coli* elevated IgG1, IgG2c, IgG2b and IgG3 antibody titres to or above the levels in mice immunized with viable *thyA*$^-$ *E. coli*. Thus, innate detection of bacterial viability leads to robust activation of a humoral adaptive response. These findings indicate that bacterial RNA can augment killed vaccines to perform as well as live ones.

Our findings reveal an inherent ability of the immune system to distinguish viable from dead microorganisms. The presence of live bacteria in sterile tissues, regardless of whether these (still) express

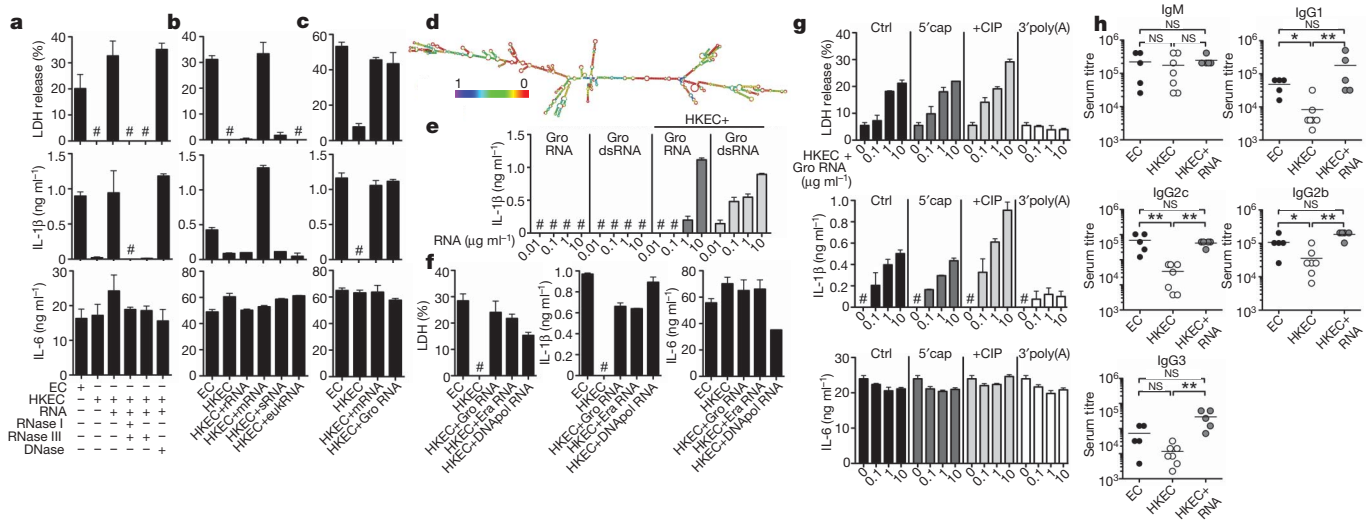

Figure 4 | Bacterial mRNA constitutes an active vita-PAMP. **a**–**c**, **e**–**g**, LDH, IL-1β and IL-6 at 24 h. **a**, Total *thyA*$^-$ *E. coli* RNA treated with RNase I and RNase III, RNase III alone, or DNase before stimulation of BMDCs. **b**, BMMs treated with viable or heat-killed *thyA*$^-$ *E. coli*, or heat-killed *thyA*$^-$ *E. coli* with 0.1 μg ml^{-1} of different bacterial RNA (ribosomal RNA (rRNA), mRNA, small RNA (sRNA) or eukaryotic RNA (eukRNA)). **c**, BMDC responses. Gro RNA indicates *in-vitro*-transcribed *E. coli* Gro operon RNA. **d**, Predicted secondary structure of Gro RNA. The colour code indicates base pairing probability. **e**, BMMs treated with *in-vitro*-transcribed Gro RNA or Gro dsRNA alone or with heat-killed *thyA*$^-$ *E. coli*. **f**, BMDC responses. Era RNA and DNApol RNA indicate *in-vitro*-transcribed *E. coli* Era GTPase and DNA polymerase III RNA, respectively. **g**, BMMs treated with different doses of unmodified (ctrl, control) or modified Gro RNA with heat-killed *thyA*$^-$ *E. coli* (5′ cap, 5′ m^7G capping; CIP, calf intestinal phosphatase; 3′ poly(A), 3′-polyadenylation). For **a**–**g**, the hash symbol indicates not detected; all RNA at 10 μg ml^{-1} except as noted; data represent ≥5 experiments. **h**, Mice vaccinated and boosted twice with viable *thyA*$^-$ *E. coli* (EC), heat-killed *thyA*$^-$ *E. coli* (HKEC) or heat-killed *thyA*$^-$ *E. coli* with 30 μg total purified bacterial RNA (HKEC+RNA) (vaccination regimen is given in Supplementary Fig. 22). Class-specific anti-*E. coli* antibody serum titres at 25 days are shown. *, $P \leq 0.05$; **, $P \leq 0.01$; ***, $P \leq 0.001$. All bars represent mean ± s.e.m.

virulence factors, poses an acute threat that must be dealt with by an aggressive immune response. Dead bacteria, on the other hand, would signify a successful immune response that can now subside. Detection of vita-PAMPs within sterile tissues signifies microbial viability. Other vita-PAMPs may exist in the form of second messengers like cyclic di-adenosine or di-guanosine monophosphates[7,28] or quorum-sensing molecules[7]. The extent to which vita-PAMPs contribute to the host response during natural infection with pathogenic bacteria, relative to other stimuli such as the activity of virulence factors, is an important issue that requires further investigation. Given that bacteria tightly regulate their virulence via multiple mechanisms in response to different environmental signals and inside a host organism during infection[29,30], detection of invariant vita-PAMPs essential to bacterial survival may be a non-redundant fail-safe strategy for host protection.

METHODS SUMMARY

Cells were infected with *E. coli* DH5α *thyA*$^-$ at a multiplicity of infection of 20 for 24 h unless stated otherwise. Supernatants were assayed for cytokines by ELISA. Genome-wide transcriptional analysis of murine bone-marrow-derived macrophages (BMMs) at 0, 1, 3 and 6 h after infection was carried out on Affymetrix GeneChip Mouse Gene 1.1 ST 24-array plates. Phagosomal leakage in BMMs was detected by measuring Fdx release using a modified method previously described[16]. In brief, BMMs were treated with *thyA*$^-$ *E. coli* in the presence of 0.167 mg ml^{-1} Fdx and imaged with excitation at 440 nm (pH insensitive) and 485 nm (pH sensitive). Fluorescence intensity ratios at 485 nm/440 nm were converted into pH maps and the percentage of Fdx release calculated (total intensity of pixels containing released Fdx/total Fdx intensity). Bacterial RNA was extracted from *E. coli* using the e.z.n.a RNA kit (Omega) and *in vitro* transcription of bacterial genes carried out using the MEGAscript kit (Ambion) followed by DNase digestion and RNA purification using the MEGAclear kit (Ambion). RNA polyadenylation was performed with the poly(A)-tailing kit (Ambion). Vaccinations were performed as a prime–boost regimen (see Methods). C57BL/6J and *P2rx7*$^{-/-}$ mice were purchased from the Jackson Laboratory. *Myd88*$^{-/-}$ and *Trif*$^{-/-}$ mice were provided by S. Akira, *Trif*$^{-/-}$×*Myd88*$^{-/-}$ by R. Medzhitov, *Nlrp3*$^{-/-}$, *Asc*$^{-/-}$ and *Nlrc4*$^{-/-}$ by Millenium, and *Casp1*$^{-/-}$ by R. Flavell. Animal care and experimentation were performed in accordance with approved MSSM Institutional Animal Care and Use Committee protocols.

Full Methods and any associated references are available in the online version of the paper at www.nature.com/nature.

Received 30 April 2010; accepted 24 March 2011.
Published online 22 May 2011.

1. Brockstedt, D. G. *et al.* Killed but metabolically active microbes: a new vaccine paradigm for eliciting effector T-cell responses and protective immunity. *Nature Med.* **11,** 853–860 (2005).
2. Cheers, C. & Zhan, Y. How do macrophages distinguish the living from the dead? *Trends Microbiol.* **4,** 453–455 (1996).
3. Detmer, A. & Glenting, J. Live bacterial vaccines—a review and identification of potential hazards. *Microb. Cell Fact.* **5,** 23 (2006).
4. Kawamura, I. *et al.* Antigen provoking gamma interferon production in response to *Mycobacterium bovis* BCG and functional difference in T-cell responses to this antigen between viable and killed BCG-immunized mice. *Infect. Immun.* **62,** 4396–4403 (1994).
5. Lauvau, G. *et al.* Priming of memory but not effector CD8 T cells by a killed bacterial vaccine. *Science* **294,** 1735–1739 (2001).
6. von Koenig, C. H., Finger, H. & Hof, H. Failure of killed *Listeria monocytogenes* vaccine to produce protective immunity. *Nature* **297,** 233–234 (1982).
7. Vance, R. E., Isberg, R. R. & Portnoy, D. A. Patterns of pathogenesis: discrimination of pathogenic and nonpathogenic microbes by the innate immune system. *Cell Host Microbe* **6,** 10–21 (2009).
8. Medzhitov, R. Approaching the asymptote: 20 years later. *Immunity* **30,** 766–775 (2009).
9. Takeuchi, O. & Akira, S. Pattern recognition receptors and inflammation. *Cell* **140,** 805–820 (2010).
10. Mariathasan, S. & Monack, D. M. Inflammasome adaptors and sensors: intracellular regulators of infection and inflammation. *Nature Rev. Immunol.* **7,** 31–40 (2007).
11. Schroder, K. & Tschopp, J. The inflammasomes. *Cell* **140,** 821–832 (2010).
12. Wing, H. J., Yan, A. W., Goldman, S. R. & Goldberg, M. B. Regulation of IcsP, the outer membrane protease of the *Shigella* actin tail assembly protein IcsA, by virulence plasmid regulators VirF and VirB. *J. Bacteriol.* **186,** 699–705 (2004).
13. Zhou, R., Yazdi, A. S., Menu, P. & Tschopp, J. A role for mitochondria in NLRP3 inflammasome activation. *Nature* **469,** 221–225 (2011).
14. Pang, I. K. & Iwasaki, A. Inflammasomes as mediators of immunity against influenza virus. *Trends Immunol.* **32,** 34–41 (2011).
15. Kanneganti, T. D. *et al.* Bacterial RNA and small antiviral compounds activate caspase-1 through cryopyrin/Nalp3. *Nature* **440,** 233–236 (2006).
16. Davis, M. J. & Swanson, J. A. Technical advance: Caspase-1 activation and IL-1β release correlate with the degree of lysosome damage, as illustrated by a novel imaging method to quantify phagolysosome damage. *J. Leukoc. Biol.* **88,** 813–822 (2010).
17. Hornung, V. *et al.* Silica crystals and aluminum salts activate the NALP3 inflammasome through phagosomal destabilization. *Nature Immunol.* **9,** 847–856 (2008).
18. Herskovits, A. A., Auerbuch, V. & Portnoy, D. A. Bacterial ligands generated in a phagosome are targets of the cytosolic innate immune system. *PLoS Pathog.* **3,** e51 (2007).
19. Shimada, T. *et al. Staphylococcus aureus* evades lysozyme-based peptidoglycan digestion that links phagocytosis, inflammasome activation, and IL-1β secretion. *Cell Host Microbe* **7,** 38–49 (2010).
20. Piekna-Przybylska, D., Decatur, W. A. & Fournier, M. J. The 3D rRNA modification maps database: with interactive tools for ribosome analysis. *Nucleic Acids Res.* **36,** D178–D183 (2008).
21. Buchmeier, N. A. & Heffron, F. Induction of *Salmonella* stress proteins upon infection of macrophages. *Science* **248,** 730–732 (1990).
22. Belasco, J. G. All things must pass: contrasts and commonalities in eukaryotic and bacterial mRNA decay. *Nature Rev. Mol. Cell Biol.* **11,** 467–478 (2010).
23. Rehwinkel, J. & Reis e Sousa, C. RIGorous detection: exposing virus through RNA sensing. *Science* **327,** 284–286 (2010).
24. Monroe, K. M., McWhirter, S. M. & Vance, R. E. Identification of host cytosolic sensors and bacterial factors regulating the type I interferon response to *Legionella pneumophila*. *PLoS Pathog.* **5,** e1000665 (2009).
25. Nallagatla, S. R., Toroney, R. & Bevilacqua, P. C. A brilliant disguise for self RNA: 5′-end and internal modifications of primary transcripts suppress elements of innate immunity. *RNA Biol.* **5,** 140–144 (2008).
26. Anderson, B. R. *et al.* Incorporation of pseudouridine into mRNA enhances translation by diminishing PKR activation. *Nucleic Acids Res.* **38,** 5884–5892 (2010).
27. Kariko, K., Buckstein, M., Ni, H. & Weissman, D. Suppression of RNA recognition by Toll-like receptors: the impact of nucleoside modification and the evolutionary origin of RNA. *Immunity* **23,** 165–175 (2005).
28. Woodward, J. J., Iavarone, A. T. & Portnoy, D. A. c-di-AMP secreted by intracellular *Listeria monocytogenes* activates a host type I interferon response. *Science* **328,** 1703–1705 (2010).
29. Gripenland, J. *et al.* RNAs: regulators of bacterial virulence. *Nature Rev. Microbiol.* **8,** 857–866 (2010).
30. Raskin, D. M., Seshadri, R., Pukatzki, S. U. & Mekalanos, J. J. Bacterial genomics and pathogen evolution. *Cell* **124,** 703–714 (2006).

Supplementary Information is linked to the online version of the paper at www.nature.com/nature.

Acknowledgements We are grateful to R. Medzhitov and J. C. Kagan for critical reading of the manuscript; C. B. Lopez for *Irf3*$^{-/-}$ mice; D. M. Monack for *Salmonella* Δ*Spi1*Δ*Spi2*; M. B. Goldberg for *Shigella* BS103; and D. A. Portnoy for *Listeria* Δ*Hly*Δ*fliC*. We thank M. Rivieccio, I. Brodsky, M. Blander, S. J. Blander, J. Sander and Blander laboratory members for insightful discussions, help and support. L.E.S. was supported by Deutsche Forschungsgemeinschaft grant SA-1940/1-1, D.A. by fellowships from the Academic Medical Center and the Landsteiner Foundation for Blood Research, and M.V.B. and M.M. by the Netherlands Nutrigenomics Centre. This work was supported by NIH grant AI080959A and the Kinship Foundation Searle Scholar award to J.M.B.

Author Contributions L.E.S. and J.M.B. designed experiments and directed the study. L.E.S. performed all experiments. M.J.D. and L.E.S. performed experiments measuring lysosomal leakage. J.A.S. helped with the design and analysis of the lysosomal leakage experiments. M.V.B. performed gene microarray analysis. M.V.B. and M.M. analysed the gene microarray data and helped with data interpretation. D.A. and J.M.B. performed experiments during the development phase of the project, and C.C.D. helped with the design of RNA-related experiments. B.R. provided bone marrow progenitor cells from *Nlrp3*$^{-/-}$, *Asc*$^{-/-}$ and *Casp1*$^{-/-}$ mice. L.E.S., D.A. and J.M.B. wrote the manuscript. J.M.B. conceived of the study.

Author Information Affymetrix Microarray data have been deposited with the NCBI Gene Expression Omnibus (http://www.ncbi.nlm.nih.gov/geo/) under accession number GSE27960. Reprints and permissions information is available at www.nature.com/reprints. The authors declare no competing financial interests. Readers are welcome to comment on the online version of this article at www.nature.com/nature. Correspondence and requests for materials should be addressed to J.M.B. (julie.blander@mssm.edu).

METHODS

Cells. Bone-marrow-derived dendritic cell (BMDC) cultures were grown as previously described[31] in RPMI 1640 supplemented with granulocyte-macrophage colony-stimulating factor (GM-CSF) and 5% fetal bovine serum (FBS), plus 100 μg ml^{-1} penicillin, 100 μg ml^{-1} streptomycin, 2 mM L-glutamine, 10 mM HEPES, 1 nM sodium pyruvate, 1% MEM non-essential amino acids, and 2.5 μM β-mercaptoethanol (all Sigma). Semi-adherent cells were harvested on ice on day 5 and re-plated immediately in fresh RPMI 1640 medium containing 10% FBS at 5×10^5 cells per well in 24-well tissue-culture-treated plates. Stimuli were added immediately after re-plating in the same medium and the cells were centrifuged for 2 min at 2,000 r.p.m. Murine macrophages were derived from the bone marrow (BMMs) of C57BL/6J, *Myd88*$^{-/-}$, *Trif*$^{-/-}$, *Trif*$^{-/-}$×*Myd88*$^{-/-}$, *Nlrp3*$^{-/-}$, *Asc*$^{-/-}$ or *Casp1*$^{-/-}$ mice, as described previously[32], in RPMI 1640 supplemented with M-CSF and 10% FBS, plus 100 μg ml^{-1} penicillin, 100 μg ml^{-1} streptomycin, 10 mM HEPES and 1 nM sodium pyruvate (all Sigma). For some experiments macrophages were derived from the bone marrow of *Irf3*$^{-/-}$ or *P2rx7*$^{-/-}$ mice. Peritoneal macrophages were harvested 72 h after intraperitoneal injection of 1 ml thioglycollate (BD Bioscience), grown overnight in RPMI 1640 medium supplemented with 10% FBS and 100 μg ml^{-1} penicillin and 100 μg ml^{-1} streptomycin, hereafter referred to as 'complete medium'. Mouse embryonic fibroblasts (MEFs) deficient for RIG-I (*RIG-I*$^{-/-}$) were provided by A. Ting with permission from S. Akira, and grown in DMEM medium containing 10% FBS and 100 μg ml^{-1} penicillin, 100 μg ml^{-1} streptomycin.

Mice. C57BL/6J and *P2rx7*$^{-/-}$ mice were purchased from Jackson Laboratories. *Myd88*$^{-/-}$ and *Trif*$^{-/-}$ mice were originally provided by S. Akira; *Myd88*$^{-/-}$ and *Trif*$^{-/-}$ mice were interbred to homozygosity to generate *Trif*$^{-/-}$×*Myd88*$^{-/-}$ mice, and were provided by R. Medzhitov. *Nlrp3*$^{-/-}$, *Asc*$^{-/-}$ or *Casp1*$^{-/-}$ bone marrow was provided by B. Ryffel and mice for *in vivo* studies were acquired from R. Flavell (through Millenium) and have been described previously[33,34]. *Irf3*$^{-/-}$ mice were provided by C. B. Lopez and were previously described[35]. We used 8–10-week-old animals for all experiments. All experiments were approved by the institutional ethics committee and carried out in agreement with the 'Guide for the Care and Use of Laboratory Animals' (NIH publication 86-23, revised 1985).

Bacteria. *Escherichia coli* K12, strain DH5α were purchased from Invitrogen. Naturally occurring thymidine auxotrophs (*thyA*$^-$) were selected on Luria-Bertani (LB) agar plates containing 50 μg ml^{-1} trimethoprim and 500 μg ml^{-1} thymidine (both Sigma). Auxotrophy was confirmed by inoculation and overnight culture of single colonies in LB medium. *thyA*$^-$ *E. coli* grew only in the presence of thymidine and were resistant to trimethoprim. For phagocytosis experiments, *thyA*$^-$ *E. coli* were grown to mid-log phase, washed three times in phosphate buffered saline (PBS) to remove thymidine and LB salts before addition to cells. For heat killing, *thyA*$^-$ *E. coli* were grown to log phase, washed and re-suspended in PBS at an optical density at 600 nm (OD_{600}) of 0.6, and subsequently incubated at 60 °C for 60 min. *thyA*$^-$ heat-killed *E. coli* were stored up to 18 h at 4 °C or used immediately after cooling. Efficient killing was confirmed by overnight plating on thymidine/trimethoprim-supplemented LB-agar plates. For gentamicin killing, *thyA*$^-$ *E. coli* were grown to mid-log phase, washed and re-suspended in LB medium containing thymidine, trimethoprim and 50 μg ml^{-1} gentamicin sulphate and incubated in a shaking incubator at 37 °C overnight. Ethanol killing was carried out by re-suspending log phase *thyA*$^-$ *E. coli* in 70% ethanol for 10 min, followed by extensive washing in PBS. For ultraviolet killing, log phase *thyA*$^-$ *E. coli* were re-suspended in PBS at an OD_{600} of 0.6, ultraviolet-irradiated with 1,000 mJ cm^{-2} in a Petri dish followed by washing with PBS. Paraformaldehyde (PFA) fixation was performed by re-suspending log-phase *thyA*$^-$ *E. coli* in 4% PFA in PBS for 10 min followed by extensive washing and re-suspension in PBS. *Shigella flexneri* virulence plasmid-cured strain BS103 was provided by M. B. Goldberg[12,36]. *thyA*$^-$ *S. flexneri* were selected similarly to *thyA*$^-$ *E. coli*. D. M. Monack provided *Salmonella enterica* serovar Typhimurium, strain SL1344 Δ*Spi1*Δ*Spi2*, lacking the *Salmonella* pathogenicity island SPI-1 and SPI-2 type-III secretion systems[37]. SL1344 Δ*Spi1*Δ*Spi2* was grown in LB medium containing 25 μg ml^{-1} kanamycin and 12 μg ml^{-1} tetracycline. *Listeria monocytogenes* Δ*Hly*Δ*fliC* lacking listeriolysin O (LLO) and flagellin expression were provided by D. Portnoy[38].

Treatment of macrophages and dendritic cells with viable and killed bacteria. Macrophages were detached and re-plated 4 h before the experiment. BMDCs were re-plated immediately before addition of bacteria or soluble ligands. Unless stated otherwise, bacteria were used at a multiplicity of infection of 20. All experiments were carried out in antibiotic-free 'complete medium'. One hour after addition of bacteria, penicillin (100 μg ml^{-1}) and streptomycin (100 μg ml^{-1}) were added to the medium to kill any remaining extracellular bacteria. Alternatively, gentamicin sulphate (50 μg ml^{-1}) was used. We also compared this approach to washing the cells and replacing the antibiotic-free medium with penicillin/streptomycin containing medium after 1 h and found no differences with regards to the cellular responses measured. Supernatants were collected 24 h after the addition of the bacteria unless stated otherwise in the figure legends.

Cytokine enzyme-linked immunosorbent assays. Supernatants from cultured BMMs or BMDCs were collected at 24 h after stimulation or at the times indicated. Enzyme-linked immunosorbent assay (ELISA) antibody pairs used for IL-6, IL-1β and TNF-α were as listed below. All ELISA antibodies were used at 2 μg ml^{-1} capture and 0.5 μg ml^{-1} detection, with the exception of IL-6 capture, which was used at 1 μg ml^{-1}. Detection antibodies were biotinylated and labelled by streptavidin-conjugated horseradish peroxidase (HRP), and visualized by the addition of *o*-phenylenediamine dihydrochloride (Sigma) (from tablets) or 3,3′, 5,5′-tetramethylbenzidine solution (TMB, KPL). Colour development was stopped with 3 M H_2SO_4 or TMB-Stop Solution (KPL), respectively. Recombinant cytokines served as standards and were purchased from Peprotech. Absorbances at 492 or 450 nm were measured, respectively, on a tunable microplate reader (VersaMax, Molecular Devices). Cytokine supernatant concentrations were calculated by extrapolating absorbance values from standard curves where known concentrations were plotted against absorbance using SoftMax Pro 5 software. Capture/detection antibody pairs were as follows. IL-6, MP5-20F3/MP5-32C11 (BDPharmingen); IL-1β, B12/rabbit polyclonal antibody (eBioscience); TNF-α, TN3-19/rabbit polyclonal antibody (eBioscience). IFN-β production was measured from supernatants using the VeriKine Mouse IFN-Beta ELISA Kit (PBL Interferon source) following manufacturer's instructions.

Anti-*E. coli* antibody ELISA. 96-well microtitre plates were coated overnight with *E. coli* lysates (3 μg ml^{-1}) that we generated from log-phase cultures of *thyA*$^-$ *E. coli*. Serum samples from immunized mice were serially diluted (12 dilutions) and incubated in the pre-coated plates for 12 h at 4 °C followed by washing and incubation with rabbit anti-mouse isotype-specific Ig–HRP (Southern Biotech) for 1 h. Bound rabbit anti-mouse Ig–HRP was visualized by the addition of *o*-phenylenediamine dihydrochloride (Sigma) from tablets, and the anti-*E. coli* antibody titres for each mouse were determined by absorbance readings at 490 nm.

Measurement of inflammatory cell death. Cell death of macrophages or BMDCs was measured using the Cytotox96 cytotoxicity assay (Promega) following manufacturer's instructions. The assay measures the release of lactate dehydrogenase (LDH) into the supernatant calculated as the percentage of total LDH content, measured from cellular lysates (100%). LDH released by unstimulated cells was used for background correction.

Flow cytometric assessment of cell death. Cells were stimulated overnight, stained for Annexin V/7AAD using the Annexin V-PE/7AAD Apoptosis Detection kit (BD Pharmingen), and analysed by flow cytometry (FACSCalibur, BD).

Flow cytometric measurement of ROS production. BMMs were loaded with the ROS indicator dye H2DCFDA (Molecular Probes/Invitrogen, 10 mM in PBS) for 30 min followed by a recovery time of 30 min in fresh pre-warmed 'complete medium'. BMMs were then stimulated with viable or heat killed *E. coli* for 60 min, washed and analysed by flow cytometry (FACSCalibur, BD).

Western blots. For detection of caspase-1, protein extracts were separated on 4–12% SDS-gradient gels (Invitrogen). For detection of all other proteins, samples were run on 10% SDS-polyacrylamide gels. Proteins were transferred to PVDF membranes (Millipore). Membranes were blocked with 5% milk in PBS and probed with the following antibodies: caspase-1 p10 (M-20)/rabbit polyclonal antibody, IκBα (C-21)/rabbit polyclonal antibody (both from Santa Cruz Biotechnologies), phospho-IRF3 (Ser 396)/rabbit polyclonal antibody, IRF3/rabbit polyclonal antibody, phospho-p38 MAPK (Thr 180/Tyr 182)/rabbit polyclonal antibody, p38 MAPK/rabbit polyclonal antibody (all from Cell Signalling Technology), α-tubulin (DM1A)/rabbit monoclonal antibody (Novus Biologicals).

Real-time PCR. Total RNA was isolated from macrophages using the RNeasy kit (Qiagen). Contaminating genomic DNA was removed by DNase digestion (DNase I, Promega). Reverse transcription was performed using Superscript III (Invitrogen) and cDNA was used for subsequent real-time PCR reactions. Quantitative real-time RT–PCR was conducted on an ABI Prism 7900 instrument using the Maxima SYBR green qPCR Master Mix (Fermentas) with the following primer pairs. β-Actin, FW 5′-GAAGTCCCTCACCCTCCCAA-3′, RV 5′-GGCATGGACGCGACCA-3′; *Il1b*, FW 5′-AAAGACGGCACACCCACCCTGC-3′, RV 5′-TGTCCTGACCACTGTTGTTTCCCAG-3′; *Ifnb*, FW 5′-GCACTGGGTGGAAT-3′, RV 5′-TTCTGAGGCATCAA-3′; *Nlrp3*, FW 5′-CGAGACCTCTGGGAAAAAGCT-3′, RV 5′-GCATACCATAGAGGAATGTGATGTACA-3′. All reactions were performed in duplicates and the samples were normalized to β-actin. 'Fold inductions' were calculated using the $\Delta\Delta C^t$ method relative to unstimulated BMMs.

Transcriptome analysis. BMMs derived from wild-type or *Trif*$^{-/-}$ mice were stimulated with viable *E. coli* for 0, 1, 3 or 6 h and total RNA was extracted using the RNeasy kit (Qiagen). RNA from three independent experiments was used for

transcriptional analysis. RNA integrity was checked on an Agilent 2100 Bioanalyser (Agilent Technologies) with 6000 Nano Chips. RNA was judged as suitable only if samples showed intact bands of 18S and 28S ribosomal RNA subunits, displayed no chromosomal peaks or RNA degradation products, and had a RNA integrity number (RIN) above 8.0.

One-hundred nanograms of RNA were used for whole-transcript cDNA synthesis with the Ambion WT expression kit (Applied Biosystems). Hybridization, washing and scanning of an Affymetrix GeneChip Mouse Gene 1.1 ST 24-array plate was carried out according to standard Affymetrix protocols on a GeneTitan instrument (Affymetrix).

Packages from the Bioconductor project, integrated in an in-house developed management and analysis database for microarray experiments, were used for analysis of the scanned arrays[39]. Arrays were normalized using the Robust Multi-array Average method[40,41]. Probe sets were defined according to ref. 42. With this method probes are assigned to unique gene identifiers, in this case Entrez IDs. The probes on the Gene 1.1 ST arrays represent 19,807 genes that have at least 10 probes per identifier. For the analysis, only genes that had an intensity value of >20 on at least two arrays were taken into account. In addition, the interquartile range of $\log_2$ intensities had to be at least 0.25. These criteria were met by 9,921 genes. Changes in gene expression are represented as signal log ratios between treatment and control. Multiple Experiment Viewer software (MeV 4.6.1) was used to create heatmaps[43,44]. Genes were clustered by average linkage hierarchical clustering using Pearson correlation. Significantly regulated genes were identified by intensity-based moderated *t*-statistics[45]. Obtained *P*-values were corrected for multiple testing by a false discovery rate method[46].

IFN-regulated genes were identified using the Interferome database (http://www.interferome.org)[47] and grouped in a heat map. Rel/NF-κB target genes were identified using another online database (http://bioinfo.lifl.fr/NF-KB/) which compiles Rel/NF-κB target genes identified by various groups[48] (http://people.bu.edu/gilmore/nf-kb/index.html). Inflammasome-related genes were compiled based on the current literature[11,49].

Measuring release from bacterial phagosomes. Measurement of fluorescein–dextran (Fdx) release from macrophage phagosomes was performed using a modified method described previously[16]. BMMs were plated onto Mat-tek coverslip dishes (MatTek Corp.) and incubated overnight. BMMs were stimulated with viable or gentamicin-killed red fluorescent protein (RFP)-expressing *thyA*$^-$ *E. coli* in the presence of 0.167 mg ml^{-1} Fdx in 200 µl of medium. After 120 min of co-culture, additional Fdx and gentamicin containing medium was added to the coverslip dishes to prevent drying and to prevent bacterial overgrowth. Cells were imaged after 2, 4 and 8 h to measure release of Fdx. Microscopic imaging was performed on an IX70 inverted microscope (Olympus) equipped with an X-cite 120 metal halide light source (EXFO) and excitation and emission filter wheels. Phase contrast and two fluorescent images were acquired for each field of cells. The fluorescent images used the same emission settings, but used different excitation band-pass filters. Fdx fluorescence intensity using an excitation filter centred at 440 nm is relatively insensitive to pH, whereas fluorescence intensity using an excitation filter centred at 485 nm is very sensitive to pH. The ratio of fluorescence intensity at 485 nm divided by 440 nm was converted to into pH maps using calibration curves generated by imaging BMMs with Fdx-containing compartments at a series of fixed pH conditions. As described previously[16], pixels with pH above 5.5 were designated as representing Fdx which has been released from endolysosomal compartments. The percentage of Fdx release was calculated by dividing the total intensity of pixels containing released Fdx by the total Fdx intensity for each cell.

Infections and vaccinations. For measurements of systemic cytokine levels, C57BL/6J wild-type, *Trif*$^{-/-}$, *Asc*$^{-/-}$ or *Nlrp3*$^{-/-}$ mice were injected with 1×10^9 viable or 5×10^9 heat-killed *thyA*$^-$ *E. coli*, respectively. Blood samples were drawn 6 h after infection, and cytokine concentrations were measured by ELISA. For determination of bacterial clearance, we infected mice with 1×10^8 viable replication-sufficient *E. coli* by intraperitoneal injection. Mice were monitored daily and moribund animals were killed according to humane criteria established and approved by our institutional IACUC committee. After 60 h, animals were killed and the spleens were explanted, homogenized, serially diluted and plated on LB-agar plates overnight followed by colony forming units (c.f.u.) counting.

For vaccinations, we followed a prime–boost regimen as shown in the schematic in Fig. 4h that was adopted from a previous study[50]. In brief, mice received an initial vaccination intraperitoneally with 5×10^7 c.f.u. of viable or heat-killed *thyA*$^-$ *E. coli* or a combination of 5×10^7 c.f.u. heat-killed *thyA*$^-$ *E. coli* and 30 µg of purified *E. coli* total RNA, followed by two boosts (5×10^6 c.f.u.) after 10 and 20 days. Polyclonal class-specific anti-*E. coli* antibody production was measured in the serum after 25 days by ELISA.

Bacterial RNA. Total bacterial RNA was isolated from *thyA*$^-$ *E. coli* using the e.z.n.a. Bacterial RNA Kit (Omega Bio-Tek), following the manufacturer's instructions. Contaminating DNA was removed by DNase digestion (TURBO DNase, Ambion/Applied Biosystems). Alternatively, total purified *E. coli* (DH5α) RNA was purchased from Ambion/Applied Biosystems, and similar results were obtained. Fractionation of bacterial RNA species was performed as follows. First, ribosomal 16S and 23S RNA (rRNA) was removed by a magnetic bead-based capture hybridization approach using the MICROBExpress kit (Ambion/Applied Biosystems). The enriched RNA was then separated into messenger RNA (mRNA) and small RNA (sRNA, including 5S rRNA) using the MEGAClear kit (Ambion/Applied Biosystems). All separated RNA fractions were precipitated with ammonium acetate and re-suspended in nuclease-free water. RNA concentration and purity were determined by measuring the absorbance at 260/280 and 260/230 nm. RNA preparations were further visualized by 1% agarose gel electrophoresis.

***In vitro* RNA transcription.** The *E. coli* Gro operon encoding the bacterial chaperonins GroEL and GroES, the GTPase Era operon or the DNA polymerase III operon were PCR amplified from genomic DNA isolated from *thyA*$^-$ *E. coli* using primer pairs containing a T7 promoter sequence (T7) in either the FW or both FW and RV primer. Gro-FWT7 5′-TAATACGACTCACTATAGGGCACCAGCCGGGAAACCACG-3′; Gro-RVT7 5′-TAATACGACTCACTATAGGAAAAGAAAAACCCCCAGACAT-3′; Gro-RV 5′-AGATGACCAAAAGAAAAACCCCCAGACATT-3′; Era-FWT7 5′-TAATACGACTCACTATAGGGCATATGAGCATCGATAAAAGTTAC-3′; Era-RV 5′-TTTAAAGATCGTCAACGTAACCGAG-3′; DNApol-FWT7 5′-TAATACGACTCACTATAGGGATGTCTGAACCACGTTTCGT-3′; DNApol-RV 5′-AGTCAAACTCCAGTTCCACCTGCTCCGAA-3′.

PCR fragments were purified using the Nucleospin Extract II PCR purification kit (Macherey-Nagel), and used as DNA templates for *in vitro* transcription. *In vitro* transcription was performed using the MEGAscript kit T7 (Ambion/Applied Biosystems) following the manufacturer's instructions. DNA templates generated with Gro-FWT7 and Gro-RV primers only contained a T7 promoter site in the sense strand and yielded single-stranded RNA, whereas PCR templates generated with Gro-FWT7 and Gro-RVT7 primers contained T7 promoter sequences in both strands, allowing transcription of two complementary strands, yielding double-stranded RNA. For generation of 5′-capped RNA, m7G(5′)ppp(5′)G cap analogue (Ambion/Applied Biosystems) was included in the transcription reaction at a GTP:cap ratio of 1:4.

RNA digestion, dephosphorylation and polyadenylation. *In-vitro*-transcribed Gro RNA, total *E. coli* RNA or *E. coli* mRNA were digested using RNase I (Promega) and RNase III (Ambion/Applied Biosystems). To remove 5′-triphosphates, RNA dephosphorylation was performed by incubating 10 µg *in-vitro*-transcribed RNA or total *E. coli* RNA or 1 mg of *E. coli* mRNA with 30 U of calf intestinal alkaline phosphatase (CIP, New England Biolabs) for 2 h at 37 °C, as described previously[51]. Polyadenylation of *in-vitro*-transcribed and purified bacterial mRNA was performed using the poly(A) Tailing kit (Ambion) following the manufacturer's instructions.

Transfection of macrophages and MEFs. For direct cytosolic delivery of total purified *E. coli* RNA or *in-vitro*-transcribed Gro RNA, 5×10^5 BMMs or 2×10^5 MEFs were transfected with 1 mg of RNA using 2 µl of Lipofectamine 2000 (Invitrogen) in 24- or 12-well plates, respectively.

Soluble ligands, inhibitors and other reagents. Lipopolysaccharide (LPS) was purchased from Sigma (*E. coli* 055:B5, phenol extracted). Caspase inhibitors z-YVAD, z-IEDT, Q-VD-OPH (all SM Biochemicals) were used at 50 µM, and added 30 min before stimulation of cells.

Statistical analysis. Statistical significances were tested by an ANOVA Kruskall–Wallis test and Bonferroni–Dunn post hoc correction. Significances are represented in the figures as follows: *, $P \leq 0.05$; **, $P \leq 0.01$; ***, $P \leq 0.001$. NS, not statistically significant; hash symbol, not detected.

31. Torchinsky, M. B., Garaude, J., Martin, A. P. & Blander, J. M. Innate immune recognition of infected apoptotic cells directs T_H17 cell differentiation. *Nature* **458,** 78–82 (2009).
32. Blander, J. M. & Medzhitov, R. Regulation of phagosome maturation by signals from toll-like receptors. *Science* **304,** 1014–1018 (2004).
33. Sutterwala, F. S. *et al.* Critical role for NALP3/CIAS1/Cryopyrin in innate and adaptive immunity through its regulation of caspase-1. *Immunity* **24,** 317–327 (2006).
34. Kuida, K. *et al.* Altered cytokine export and apoptosis in mice deficient in interleukin-1β converting enzyme. *Science* **267,** 2000–2003 (1995).
35. Sato, M. *et al.* Distinct and essential roles of transcription factors IRF-3 and IRF-7 in response to viruses for IFN-α/β gene induction. *Immunity* **13,** 539–548 (2000).
36. Maurelli, A. T., Baudry, B., d'Hauteville, H., Hale, T. L. & Sansonetti, P. J. Cloning of plasmid DNA sequences involved in invasion of HeLa cells by *Shigella flexneri*. *Infect. Immun.* **49,** 164–171 (1985).
37. Haraga, A., Ohlson, M. B. & Miller, S. I. Salmonellae interplay with host cells. *Nature Rev. Microbiol.* **6,** 53–66 (2008).
38. Schnupf, P. & Portnoy, D. A. Listeriolysin O: a phagosome-specific lysin. *Microbes Infect.* **9,** 1176–1187 (2007).
39. Gentleman, R. C. *et al.* Bioconductor: open software development for computational biology and bioinformatics. *Genome Biol.* **5,** R80 (2004).

40. Bolstad, B. M., Irizarry, R. A., Astrand, M. & Speed, T. P. A comparison of normalization methods for high density oligonucleotide array data based on variance and bias. *Bioinformatics* **19,** 185–193 (2003).
41. Irizarry, R. A. *et al.* Summaries of Affymetrix GeneChip probe level data. *Nucleic Acids Res.* **31,** e15 (2003).
42. Dai, M. *et al.* Evolving gene/transcript definitions significantly alter the interpretation of GeneChip data. *Nucleic Acids Res.* **33,** e175 (2005).
43. Saeed, A. I. *et al.* TM4: a free, open-source system for microarray data management and analysis. *Biotechniques* **34,** 374–378 (2003).
44. Saeed, A. I. *et al.* TM4 microarray software suite. *Methods Enzymol.* **411,** 134–193 (2006).
45. Sartor, M. A. *et al.* Intensity-based hierarchical Bayes method improves testing for differentially expressed genes in microarray experiments. *BMC Bioinformatics* **7,** 538 (2006).
46. Storey, J. D. & Tibshirani, R. Statistical significance for genomewide studies. *Proc. Natl Acad. Sci. USA* **100,** 9440–9445 (2003).
47. Samarajiwa, S. A., Forster, S., Auchettl, K. & Hertzog, P. J. INTERFEROME: the database of interferon regulated genes. *Nucleic Acids Res.* **37,** D852–D857 (2009).
48. Pahl, H. L. Activators and target genes of Rel/NF-κB transcription factors. *Oncogene* **18,** 6853–6866 (1999).
49. Coll, R. C. & O'Neill, L. A. New insights into the regulation of signalling by toll-like receptors and nod-like receptors. *J. Innate Immun.* **2,** 406–421 (2010).
50. Lim, S. Y., Bauermeister, A., Kjonaas, R. A. & Ghosh, S. K. Phytol-based novel adjuvants in vaccine formulation: 2. Assessment of efficacy in the induction of protective immune responses to lethal bacterial infections in mice. *J. Immune Based Ther. Vaccines* **4,** 5 (2006).
51. Hornung, V. *et al.* 5′-Triphosphate RNA is the ligand for RIG-I. *Science* **314,** 994–997 (2006).